

Promotional effect of magnesia addition to active carbon supported Pd catalyst on the characteristics and hydrodechlorination activity of CCl_2F_2

J. Krishna Murthy, S. Chandra Shekar, A.H. Padmasri, A. Venugopal, V. Siva Kumar, B.M. Nagaraja, V. Shashikala, B. David Raju, P. Kanta Rao, K.S. Rama Rao *

Catalysis and Physical Chemistry Division, Indian Institute of Chemical Technology, Hyderabad 500 007, India

Received 26 August 2003; accepted 17 November 2003

Published online: 29 January 2004

Abstract

Magnesia modified active carbon supported palladium (Pd–MgO/C) catalyst prepared by co-impregnation, has shown superior activity in the hydrodechlorination of CCl_2F_2 to produce CH_2F_2 in greater yields compared to Pd/C and Pd/MgO catalysts. The high activity of Pd–MgO/C catalyst is due to the synergistic effect of Pd/C and Pd/MgO components. CO chemisorption results indicate the formation of bigger particles of Pd in Pd–MgO/C catalyst and the formation of MgF_2 from MgO (on reaction with HF released during the reaction), induce electron deficient surface so that the rate of the desorption of intermediate CF_2^* adsorbed species is more facile yielding CH_2F_2 .

© 2003 Elsevier B.V. All rights reserved.

Keywords: Pd–MgO/C catalyst; Hydrodechlorination; Synergistic effect

1. Introduction

The ozone destructive nature of chlorofluorocarbons (CFCs) [1] and the severe sanctions on their production and usage under Montreal protocol resulted in searching methodologies for the safe disposal of CFCs. Hydrodechlorination of CFCs is rated as one of the best among all the CFC disposal methods as it yields hydrochlorofluorocarbons (HCFCs) and/or hydrofluorocarbons (HFCs) [2–6]. Difluoromethane (HFC-32) with zero ozone depletion potential (ODP) and having properties very close to a deep refrigerant is an excellent example that can be produced by the hydrodechlorination of CFC-12 [2].

Palladium has been the preferred active phase in supported catalysts for selective hydrodechlorination of CFCs. Several studies have been focused on the role of

support [2,5–12] and the influence of a second metal/metal oxide as a promoter [3,7,13–17] in achieving high CCl_2F_2 conversion and CH_2F_2 selectivity. Addition of a second metal ion (to supported Pd catalyst), which is not easily reducible at the reaction temperature, may yield interesting results in the hydrodechlorination of CCl_2F_2 through modification of active phase.

Pd/C is the widely investigated catalyst in the synthesis of HFCs. However, high hydrogenation activity of carbon supported Pd catalysts are generally associated with low selective dechlorination and a small increase in the reaction temperature may lead to high selectivity towards the formation of fully hydrogenated products, i.e., methane. Pd/C catalyst systems wherein Pd dispersion is found to be quite high give smaller particles thereby resulting in the higher selectivity towards methane, which is an undesired product. There are only few reports available for the hydrodechlorination of CFCs over Pd supported on basic catalysts [15,16,18,19]. The reason may be the low resistance expected to be offered by these catalysts towards the

* Corresponding author.

E-mail address: kshamarao@iict.ap.nic.in (K.S. Rama Rao).

corrosive reaction conditions during the course of reaction. But, the reports on hydrodechlorination of carbon tetrachloride (CCl_4) over Pt/MgO [17] and hydrodechlorination of CCl_2F_2 over Pd/MgF₂ [18] have indicated that these catalysts are very stable during the reaction conditions. More recently Coq and co-workers [19] have shown that Pd supported Mg–Al hydrotalcite precursors to be active and selective in the synthesis of CH_2F_2 by hydrogenolysis of CCl_2F_2 . In our earlier studies [5,6] we found stable activity and high selectivity towards CH_2F_2 in the hydrodechlorination of CCl_2F_2 over Pd/MgO and Pd supported on hydrotalcite precursors.

In order to halt full hydrogenation ability and to improve the selectivity towards HFC-32 on Pd/C catalysts, an attempt has been made to modify the characteristics of Pd/C to some extent by the incorporation of small amounts of magnesia. Thus, the basis for the selection of modified carbon supports is to develop a new class of Pd based catalysts with the combined characteristics of carbon and magnesia.

2. Experimental

Pd/C and Pd/MgO catalysts are prepared by impregnation of activated carbon (M/s Norit; BET surface area: $960 \text{ m}^2 \text{ g}^{-1}$ and MgO (MgO is prepared by the precipitation of $\text{Mg}(\text{OH})_2$ from aqueous solution of $\text{Mg}(\text{NO}_3)_2$ with dilute aqueous solution of NaOH as the precipitating agent at pH 10–11 and the resulting gel is filtered and washed thoroughly with warm distilled water to remove excess Na^+ ion and then dried in oven at 110°C overnight and calcined in air/ $500^\circ\text{C}/18 \text{ h}$) with acidified aqueous solution containing requisite amount of PdCl_2 to give a Pd loading of 4 wt%. Pd–MgO/C catalyst is prepared by co-impregnation of activated carbon support with acidified aqueous solution containing requisite amounts of PdCl_2 and $\text{Mg}(\text{NO}_3)_2$ to give a Pd loading of 4 wt% and a Mg content of 10 wt% as MgO. After evaporating excess solution on a water bath, all the impregnated catalysts are oven dried at 120°C for 12 h. Prior to impregnation, the activated carbon has been purified by (i) boiling in dil. HNO_3 (ii) washing with de-ionized water (iii) treating with hot dil. NH_4OH and (iv) washing with de-ionized water in sequential manner for three times and then dried for 24 h at 100°C . BET-surface area of the reduced catalyst samples is measured by nitrogen adsorption at -196°C using an all glass high vacuum unit at 10^{-6} Torr.

XRD analysis of fresh and used catalyst samples are carried out on a Siemens D5000 X-ray diffractometer using $\text{Cu K}\alpha$ radiation. TPR studies are made on an on-line system which consists of a reactor placed in a metal block furnace equipped with a temperature programmer cum controller connected with a thermocouple and the

reactor outlet is connected to a GC, equipped with thermal conductivity detector and a data station with a standard GC software for recording the TPR profiles. In a typical experiment, about 200 mg of catalyst sample (18/25 BSS mesh particles) is placed in the reactor and heated linearly at a ramp of $11^\circ\text{C}/\text{min}$ (for Pd/MgO catalysts, $5^\circ\text{C}/\text{min}$) from ambient temperature to 700°C and kept isothermal at that temperature for 30 min while passing the reducing gas mixture (6% H_2 in argon) over the catalyst. The gas mixture from the outlet of the reactor is passed through a dilute alkali (KOH) trap to remove HCl/HF, the by-products of the reaction, followed by a molecular sieve trap to remove the moisture and then let into the GC blank column. The KOH trap is equipped with a conductivity cell connected to a conductivity meter to monitor the conductivity changes due to the formation of KCl or KF (reaction between KOH in the trap and HCl and/or HF released in the hydrodehalogenation of CCl_2F_2 reaction). CO pulse-chemisorption experiments are performed by dynamic pulse-flow using a Data Cat system consisting of a micro quartz reactor (o.d. 10 mm) that can be heated electrically in a metal block furnace, the temperature of which is monitored by a PID temperature controller cum programmer. The outlet of the reactor is connected to the GC, equipped with a thermal conductivity detector (TCD), which in turn is connected to the data station for recording and analyzing the evolution of the desorbed gas. In a typical experiment, ~ 100 mg of catalyst is taken in the reactor and reduced in H_2 flow at 400°C for 2 h, then the catalysts are flushed with He for 1 h at the same temperature. After flushing, the temperature is brought down to 30°C (room temperature), followed by injecting CO (using 10% CO balance helium mixture) in pulses through a six-port valve having a loop of $500 \mu\text{L}$. The change in the concentration of CO due to the adsorption by the catalyst indicate a respective change in the TCD signal due to the change in the conductivity and this change in the form of differential pattern has been recorded in the data station. By calculating the cumulative volume for each pulse a graph is plotted for the pulse number against cumulative volume. The extrapolated line on the y-axis will give the chemisorbed volume.

All the supported Pd catalysts are evaluated for their hydrogenolysis activity in a micro-flow on-line reactor interfaced with a GC (Sigma Instruments, India) equipped with TCD and FID through a six port sampling valve having a loop of 1 ml volume. About 1 g of the catalyst is placed in the micro flow reactor and reduced in hydrogen flow ($40 \text{ ml}/\text{min}$) at a temperature of 400°C , for 4 h. The reactor is then cooled to the reaction temperature under hydrogen flow and CFC-12 feed and hydrogen are passed on to the catalyst bed along with nitrogen (to maintain required gas hourly space velocity (GHSV)). The product mixture, before entering

the GC, is scrubbed with an aq. alkali (4% KOH) solution to remove HCl/HF that are produced during the course of reaction. The product mixture is then analyzed at regular time intervals using a GC with FID detector and Porapak-Q column (3 m length, 3 mm dia., SS) at an oven temperature of 120 °C. The identification of major products is done by GC-MS (Varian-7070) Micro Mass-Spectra unit, comparing the m/e values with standard m/e values reported by Simmonds et al. [20]. The major components of product mixture are found to be HFC-32, CH₄ (combined selectivity ~90%) and unreacted CFC-12. The minor components (combined selectivity ~10%) are found to be HFC-41 and HCFC-22 depending on the reaction conditions.

3. Results and discussion

3.1. BET-surface area and XRD results

The BET-surface areas of the fresh catalysts are presented in Table 1. The impregnation of Pd resulted in the reduction of the surface area of activated carbon from 960 to 586 m² g⁻¹ with Pd occupying some of the surface of the carbon. The addition of MgO to Pd/C catalyst, however, resulted in the increase in the surface area of the Pd–MgO/C catalyst from 586 to 718 m² g⁻¹. The surface area of Pd–MgO/C catalyst is definitely lower compared to that of pure support indicating the blockage of pores of active carbon by both Pd and MgO species. However, The extra area generated upon addition of MgO to Pd/C catalyst might be due to either smaller crystallites of MgO or the Pd–MgO interacted species. Since the precursor for Pd deposition is PdCl₂ with small amount of HCl (used for the purpose of PdCl₂ solubility), one can expect an interaction between MgO and Cl⁻ ion. The Pd/MgO catalyst showed a very low surface area as compared to that of carbon supported Pd catalyst. However, the support MgO possesses lower surface area than that of carbon. XRD patterns of the reduced and used Pd/C, Pd/MgO and Pd–MgO/C catalysts are shown in Fig. 1. In MgO supported Pd catalysts phases of MgO (ASTM Card No. 4-0829) are seen. No signals due to PdCl₂ are observed from these patterns. This indicates that PdCl₂ in

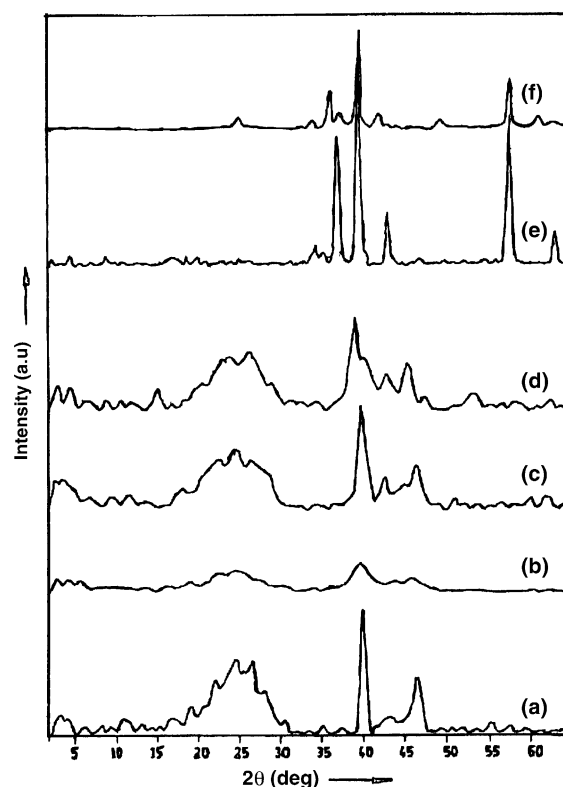


Fig. 1. XRD patterns of the reduced and used catalysts of Pd/C, Pd–MgO/C and Pd/MgO. (a) Pd/C – reduced; (b) Pd/C – used; (c) Pd–MgO/C – reduced; (d) Pd–MgO/C – used; (e) Pd/MgO – reduced; (f) Pd/MgO – used.

these catalysts are reduced to metallic Pd. Signals due to α -Pd phase ($2\theta = 40^\circ$ with “ d ” value of 2.25 Å, $2\theta = 46.5^\circ$ with “ d ” value of 1.95 Å and $2\theta = 67.9^\circ$ with “ d ” value of 1.38 Å, ASTM card No. 5-0681) are observed in these catalysts. In the used Pd/MgO and Pd–MgO/C catalyst PdC_x phase ($2\theta = 39.5^\circ$ with “ d ” value of 2.303 Å, $2\theta = 45.5^\circ$ with “ d ” value of 1.991 Å and $2\theta = 66.5^\circ$ with “ d ” value of 1.405 Å) and α -Pd phase are observed. Juszczak et al. [7] have reported the presence of PdC_x phases in used catalysts after hydrodechlorination of CCl₂F₂ over Pd/Al₂O₃. Phases due to MgO and MgF₂ ($2\theta = 27.2^\circ$ with “ d ” value of 3.28 Å, $2\theta = 40.4^\circ$ with “ d ” value of 2.23 Å and $2\theta = 53.5^\circ$ with “ d ” value of 1.71 Å, ASTM card No. 41-1443) are observed in both Pd/MgO and Pd–MgO/C used catalysts. Transformation of oxidic support during the hydrodechlorination process due to the evolution of HCl and HF during the course of the reaction is well reported [2]. Kanta Rao and co-workers [21] and Hess and co-workers [22] have reported the transformation of catalyst material into metal oxy/hydroxy fluorides during dismutation reaction of CCl₂F₂. The XRD patterns of reduced Pd/C catalyst clearly indicate the presence of α -Pd phase, whereas in used catalysts, the α -Pd phase with lower intensity compared to those of the corresponding reduced catalyst sample is found.

Table 1
Physical characteristics of the catalysts

Catalyst	BET-SA ^a (m ² g ⁻¹)	CO-uptake (mmol g ⁻¹)	% Dispersion	Particle size (nm)
C	960	–	–	–
Pd/C	586	32.0	8.5	1.4
Pd/MgO	56	6.4	1.7	6.7
Pd–MgO/C	718	4.0	1.1	10.4

^a BET-surface areas of fresh catalysts.

3.2. CO pulse-chemisorption

The CO-uptakes of the catalysts measured by pulse chemisorption method are presented in Table 1. The percentage dispersion of Pd calculated from these uptakes show that although Mg modified Pd supported on carbon has exhibited extra BET-surface area, the CO uptake is the least when compared to Pd/C and Pd/MgO catalysts. One probable reason may be the coverage or interaction of Mg with the Pd on the surface. Thus correspondingly the dispersion of Pd is the least over Pd–MgO/C catalyst attributed to the formation of bigger particles of Pd over this catalyst. High activity over this catalyst is expected compared to the other catalysts because of the formation of bigger particles of Pd since Coq et al. [2] have shown the catalysts with bigger particles of Pd to form CH_2F_2 more selectively. No significant amount of CO uptake has been observed on activated carbon support. It is in agreement with the literature [23].

3.3. TPR results

Temperature programmed reduction (TPR) patterns (Fig. 2) reveal different features. The reduction process related to Pd during the TPR run are:

- (i) $\text{PdCl}_2 + \text{H}_2 \rightarrow \text{Pd}^0 + 2\text{HCl}$
at room temperature on Pd/C
- (ii) $\text{PdO} + \text{H}_2 \rightarrow \text{Pd}^0 + \text{H}_2\text{O}$
at 160 °C on calcined Pd/MgO

TPR pattern of Pd/C exhibits two positive signals centered at a T_{max} of ~ 650 °C due to the gasification of carbon and the other centered at a T_{max} of ~ 250 °C on account of the hydrogen consumption corresponding to the evolution of HCl formed by the reaction of adsorbed Cl^* on the catalyst surface with hydrogen [11]. The evolution of HCl at this temperature is also evidenced from the change in the conductivity of the KOH solution in the trap placed at the outlet of the reactor in the TPR run (Fig. 3). The H_2 consumption in TPR pattern (for the reaction between H atoms generated through spill over mechanism and Cl^- adsorbed species) can be explained on the basis of spill over mechanism [24,25]. It is reported that active carbon support possesses a variety of functional groups like COOH, lactonic, OH groups, etc. [25–27], which may be responsible for the stabilization of Cl^- species. The decrease in the conductivity due to evolution of HCl which reacts with KOH forming KCl can be observed from the conductivity pattern (Fig. 3). Thus, one can believe that Cl^- ion stabilized on carbon support and spill over H on the support react together to form HCl which is indicated by a change in the conductivity value. This reaction occurred at a temperature of 250 °C, where H_2 consumption from TPR patterns (with TCD detector) is also observed. No negative peak corresponding to β -

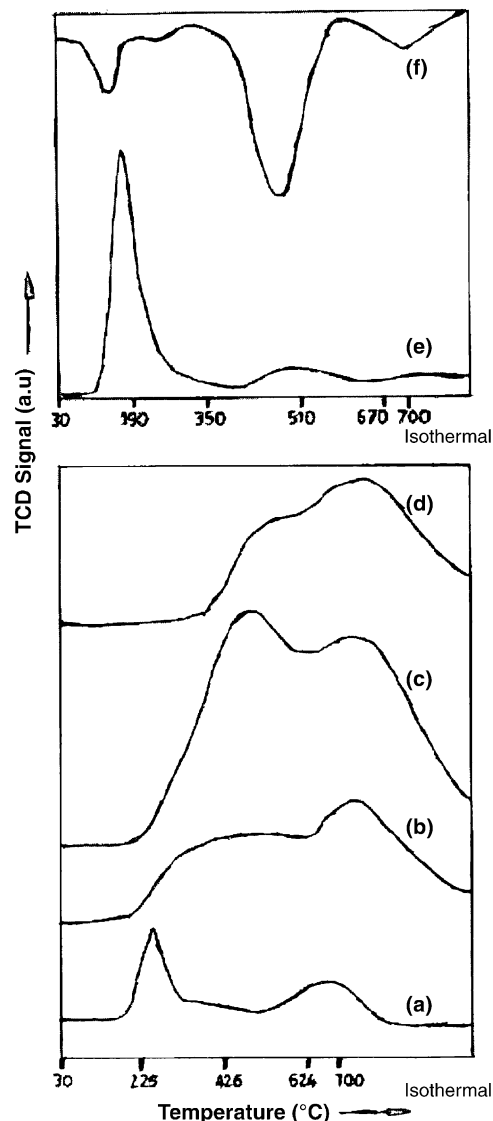


Fig. 2. TPR profiles of the fresh and used catalysts of Pd/C, Pd–Mg/C and Pd/MgO. (a) Pd/C – fresh; (b) Pd/C – used; (c) Pd–MgO/C – fresh; (d) Pd–MgO/C – used; (e) Pd/MgO – fresh; (f) Pd/MgO – used.

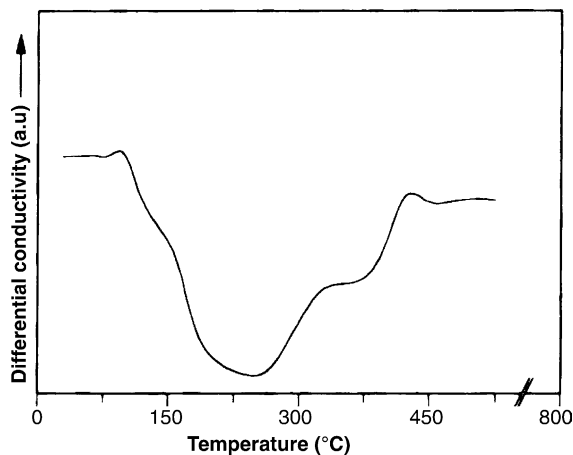


Fig. 3. Electrical conductivity pattern (during TPR run) of Pd/C catalyst.

PdH_x decomposition is observed over Pd/C fresh catalysts. It is a known fact that PdCl₂ on carbon gets reduced at room temperature (according to step (i)). According to Kutty and Vannice [28,29] in Pd supported on active carbon, suppression of β-PdH_x formation is due to carbon contamination of the surface and bulk Pd (reduction of Pd particle size). The other reason for the absence of β-PdH_x is due to the high dispersion of Pd on activated carbon because of high surface area of the support. The used Pd/C catalysts showed a positive peak around 450 °C which may be attributed to the evolution of hydrocarbons from the reduction of CH_x (x ≥ 2) species formed on the surface of the catalyst during the course of the reaction [30]. The peak corresponding to gasification of carbon is also observed at a temperature of 700 °C in the Pd/C used catalyst.

No negative peak corresponding to β-PdH_x decomposition is observed over Pd/MgO fresh catalysts. One probable reason may be the high dispersion of Pd over MgO. Increase in dispersion of Pd in Pd/SiO₂ system or decrease in Pd crystallite size is reported to result in the decrease in the intensity of β-PdH_x decomposition peak [31]. A strong positive peak with a T_{max} at ~160 °C is observed in calcined fresh catalysts of Pd/MgO with a shoulder ~270 °C. This peak probably corresponds to PdO reduction (according to step (ii)) and/or to hydrogen consumption for the formation of metallic Pd (formed during the reduction of PdCl₂ which gets reduced at room temperature in hydrogen atmosphere) and/or hydrogen adsorption directly on MgO [6,32,33]. A negative peak centered at ~400 °C can be seen from the TPR pattern of the fresh catalyst which may be attributed to the partial desorption of hydrogen that is chemisorbed on both palladium and magnesia [34]. Since the intensity of this peak is very small compared to the positive signal at a T_{max} of ~160 °C, it is not clearly visible from this pattern. The high temperature positive peak above 500 °C shows further consumption of hydrogen which may be attributed to the spill over of the hydrogen activated on metallic Pd on to the MgO support [35]. The TPR patterns of used Pd/MgO catalysts (Fig. 2) show a negative peak centered at ~100 °C.

This peak is attributed to the decomposition of β-PdH_x [30]. Negative signal centered at T_{max} ~ 450 °C is found in used Pd/MgO catalysts. Also signal centered at a T_{max} of 680 °C is present in this catalyst. These peaks may be attributed to the evolution of methane confirmed from FID pattern of the TPR reactor outlet stream (not shown in figure) particularly by the reduction of coke moieties (CH_x ≥ 2) present on the catalyst surface. Deshmukh and d'Itri [30] have reported the presence of surface CH₂ species in the used Pd/AlF₃ catalysts.

The combined characteristics of Pd/C and Pd/MgO catalysts can be seen from the TPR signals of Pd–MgO/C catalyst. Thus in Pd–MgO/C catalyst, the signal at a T_{max} of 500 °C may be due to consumption of hydrogen

which may be attributed to the spill over of the hydrogen activated on metallic Pd on to the MgO support [35] or to the hydrogen consumption corresponding to some interaction of Pd–MgO over carbon. However, no such interacted species of Pd–MgO is observed from X-ray diffraction analysis. But the absence of the β-PdH_x decomposition peak and the peak around 160 °C corresponding to PdO reduction that is observed over Pd/MgO fresh catalyst clearly indicates that Pd is highly dispersed state as well as in some interacted form with MgO. There is a shift in the T_{max} of the peak corresponding to the hydrogen consumption for the gasification of carbon to ~700 °C from 650 °C observed over Pd/C catalyst. The TPR patterns of used Pd–MgO/C catalyst showed similar pattern to its fresh catalyst except for the lowering of the intensity of the peak at T_{max} at 500 °C probably corresponding to the partial transformation of MgO to MgF₂ phase during the course of the reaction. No signal corresponding to any hydrocarbon evolution is seen over the used catalyst of Pd–MgO/C unlike the used Pd/C and Pd/MgO catalysts. This suggests that there is a negligible amount of coking taking place over the Pd–MgO/C catalyst.

3.4. Activity data

The product composition during hydrodechlorination of CCl₂F₂ against time on stream, on various catalysts studied at 260 °C is shown in Table 2. Pd–MgO/C catalyst exhibited good activity and selectivity compared to that of the Pd/MgO and Pd/C catalysts. In the case of Pd/C catalyst, even though the conversion remains constant at 100% at all the time; there is a decrease in the selectivity towards CH₂F₂ with time. Pd/MgO catalyst shows an increasing trend both in conversion of CCl₂F₂ and in the selectivity towards CH₂F₂ against time on stream. The activity (in terms of conversion of CCl₂F₂ and selectivity to CH₂F₂) of Pd/MgO/C catalyst remains

Table 2
CCl₂F₂ hydrodechlorination activity data against time on stream

Catalyst	Time (min)	%Conversion of CCl ₂ F ₂	%Selectivities		
			CH ₂ F ₂	CH ₄	Others ^a
Pd/C	60	100	30	47	23
	120	100	23	56	21
	180	100	22	60	18
Pd–MgO/C	60	66.5	76	23	2
	120	66.1	75	22	3
	180	66.0	75	22	3
Pd/MgO	60	35.0	40	55	5
	120	40.0	56	42	2
	180	58.0	64	30	6

Reaction conditions: catalyst wt, 1.0 g; H₂/CFC-12 = 8; (H₂ + CFC-12) flow = 3.78 l per hour; reaction temperature = 260 °C.

^a Others = CHClF₂, CH₃F, CHCl₃F.

constant at all the timings and the yield of CH_2F_2 is higher compared to other two catalysts. In addition to CH_4 formation, other products like CHClF_2 , CH_3F , and CHCl_2F are also formed in high concentrations on Pd/C catalyst compared to the other two catalysts. However, on Pd/C and Pd–MgO/C catalysts, at a reaction temperature of 220 °C, the CCl_2F_2 conversions are 71% and 28% and the CH_2F_2 selectivities are 30% and 82%, respectively. Thus at lower reaction temperatures, the yield of CH_2F_2 on both Pd/C and Pd–MgO/C is more or less same. The high conversion of CCl_2F_2 over Pd/C catalyst can be attributed to the higher Pd dispersion on C. But, the selectivity towards HFC-32 is lower on this catalyst, indicating that the high dispersed Pd catalysts are highly active towards the complete dehalogenation forming CH_4 . It does not mean that all the low Pd dispersed catalysts are active for the selective dechlorination. An optimum particle size of Pd is always needed for the dechlorination process. In addition to the optimum particle size of Pd (as it appears from Pd–MgO/C), the electron deficient environment of Pd created by the incorporation of MgO (which has been transformed into MgF_2 during the reaction) is the necessary condition for obtaining good yields of HFC-32. Effect of reaction temperature in the hydrodechlorination of CCl_2F_2 over Pd–MgO/C catalyst is shown in Fig. 4.

The reaction has been studied in the temperature range of 180–320 °C. The main products observed are CH_2F_2 and CH_4 along with the formation of the other products like CHClF_2 and CH_3F and at higher temperatures above 250 °C, the formation of other by-products like CHCl_2F and trace amounts of Cl/F exchange type products are also observed. %Conversion of CCl_2F_2 increased from around 5% to >90% with increase in reaction temperature from 180 to 320 °C.

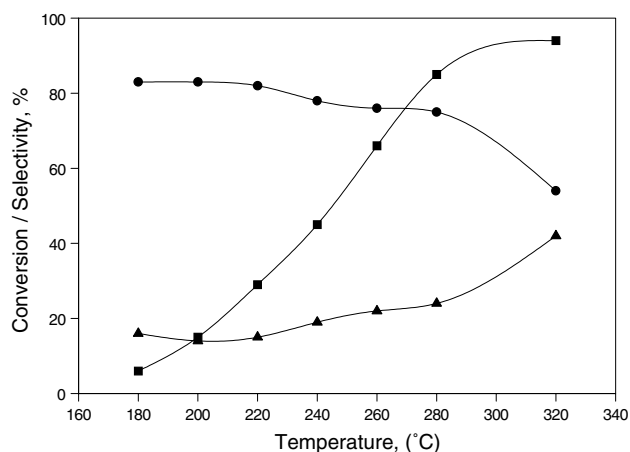


Fig. 4. Effect of reaction temperature in the hydrodechlorination of CCl_2F_2 over Pd–MgO/C catalyst at a GHSV = 4800 h^{-1} and $\text{H}_2/\text{CCl}_2\text{F}_2 = 8$. (■) Conversion of CCl_2F_2 ; (●) selectivity of CH_2F_2 ; (▲) selectivity of CH_4 .

The selectivity to CH_2F_2 is more or less constant till 260 °C and beyond this drastically decreased and a corresponding increase in selectivity to CH_4 is observed with the increase in reaction temperature. However, 260 °C seems to be the optimum reaction temperature as the %selectivity towards CH_2F_2 is found to be reasonably good at this reaction temperature. At this reaction temperature, although Pd/C gave 100% conversion, the selectivity to the desired product is much low as compared to Pd/MgO and Pd–MgO/C catalysts. Thus, Pd–MgO/C is found to be superior for yielding CH_2F_2 more selectively as compared to Pd/MgO and Pd/C catalyst. It is observed from this figure that even though there is decrease in the selectivity towards CH_2F_2 beyond 260 °C, the yield of CH_2F_2 is higher at 280 °C.

The higher selectivity to CH_2F_2 over Pd/MgO or Pd/MgF₂ catalysts may be explained on the basis of the mechanism proposed by Coq et al. [2] that the Lewis acidity of the MgF_2 support similar to that over AlF_3 makes Pd more electron deficient thus enhancing the selectivity towards CH_2F_2 through easier desorption of the CF_2^* species. In the hydrodehalogenation of CF_2Cl_2 , the most abundant surface intermediate would be $^*\text{CF}_2$ radical. The selectivity for the two main products, i.e., CH_2F_2 and CH_4 is mainly determined by the ratio between the desorption rate of $^*\text{CF}_2$ assisted with hydrogen to give CH_2F_2 and the rate of the surface reaction leading to CH_4 . The desorption of $^*\text{CF}_2$ assisted by H_2 will be easier if the bond between CF_2 and Pd is weak. In Pd= CF_2 bond, the $^*\text{CF}_2$ radical is electron withdrawing due to inductive effect of fluorine atoms and, therefore, the metal carbon bond will be weak if Pd becomes more electron deficient. The lower electron density of the Pd favors the desorption of $^*\text{CF}_2$, the most abundant surface intermediate, and hence the selectivity to CH_2F_2 . The presence of F^- in Pd/MgO and Pd–MgO/C makes Pd more electron deficient. Pd/C gives higher conversion of CCl_2F_2 but low selectivity towards the desired product CH_2F_2 . Incorporation of MgO into Pd/C system enhanced the selectivity towards CH_2F_2 and also improved the yield towards this product as compared to Pd/MgO system. Further the co-impregnation of Pd and Mg over C has facilitated a better interaction of Pd and Mg giving much higher selectivity to CH_2F_2 . Pd–MgO/C system hence incorporates the good qualities of both Pd/C and Pd/MgO catalysts for the selective synthesis of CH_2F_2 by the hydrodechlorination of CCl_2F_2 .

Incorporation of MgO into Pd/C system helps in the enhancement of the yield towards CH_2F_2 in the hydrodechlorination of CCl_2F_2 . Conversion of MgO into MgF_2 during the reaction facilitated in increasing the electron deficient environment on Pd surface there by increasing CH_2F_2 selectivity. Low amount of coking (as observed from the TPR patterns of used Pd–MgO/C catalysts) is one of the main advantages of this catalyst.

The synergistic effect between Pd/MgO and Pd/C seems to be the main reason for the high activity of Pd–MgO/C catalyst.

Acknowledgements

The authors thank Dr. J.S. Yadav, Director, ICT, Hyderabad, India for his cooperation and keen interest in this work. J.K.M., S.C. and A.H.P. thank the Council of Scientific and Industrial Research, India and University Grants Commission, India for the award of the research fellowships.

References

- [1] M.J. Molina, F.S. Rowland, *Nature* 249 (1974) 810.
- [2] B. Coq, J.M. Cognion, F. Figueras, D. Tournigant, *J. Catal.* 141 (1993) 21.
- [3] R. Ohnishi, W.L. Wang, M. Ichikawa, *Appl. Catal. A* 113 (1994) 29.
- [4] S. Chandra Shekar, A. Venugopal, K.S. Rama Rao, P.S. Sai Prasad, R. Srinivas, P. Kanta Rao, *Stud. Surf. Sci. Catal.* 113 (1993) 391.
- [5] A.H. Padmasri, A. Venugopal, J. Krishna Murthy, P. Kanta Rao, K.S. Rama Rao, *J. Mol. Catal.* 181 (2002) 73.
- [6] A.H. Padmasri, A. Venugopal, J. Krishna Murthy, K.S. Rama Rao, P. Kanta Rao, G. Kishan, J.W. Niemantsverdriet, *J. Phys. Chem. B* 106 (2002) 1024.
- [7] W. Juszczuk, A. Malinowski, Z. Karpinski, *Appl. Catal. A* 166 (1998) 311.
- [8] B. Coq, F. Figueras, S. Hub, D. Tournigant, *J. Phys. Chem.* 99 (1995) 11159.
- [9] K. Early, V.I. Kovalchuk, F. Lonyi, S.S. Deshmukh, J.L. d'Itri, *J. Catal.* 182 (1999) 219.
- [10] P.S. Sai Prasad, N. Lingaiah, S. Chandra Shekar, K.S. Rama Rao, P. Kanta Rao, K.V. Raghavan, F.J. Berry, L.E. Smart, *Catal. Lett.* 66 (2001) 201.
- [11] A. Wiersma, E.J.A.X. van de Sandt, M.A. den Hollander, H. van Bekkum, M. Makkee, J.A. Moulijn, *J. Catal.* 177 (1998) 29.
- [12] M. Makkee, E.J.A.X. van de Sandt, A. Wiersma, J.A. Moulijn, *J. Mol. Catal.* 134 (1998) 134.
- [13] B. Coq, S. Hub, F. Figueras, D. Tournigant, *Appl. Catal. A* 101 (1993) 41.
- [14] R. Ohnishi, I. Suzuki, M. Ichikawa, *Chem. Lett.* (1991) 841.
- [15] M.J. Sweetman, J. Thomson, *J. Chem. Soc., Chem. Commun.* (1994) 2385.
- [16] A. Malinowski, W. Juszczuk, J. Pielaszek, M. Bonarowska, Z. Karpinski, *J. Chem. Soc., Chem. Commun.* (1999) 685.
- [17] M. Bonarowska, A. Malinowski, W. Juszczuk, Z. Karpinski, *Appl. Catal. B* 30 (2001) 187.
- [18] S.Y. Kim, H.C. Choi, O.B. Yang, K.H. Lee, J.S. Lee, Y.G. Kim, *J. Chem. Soc., Chem. Commun.* (1995) 2169.
- [19] A. Morato, C. Alonso, F. Medina, Y. Cesteros, P. Salarge, J.E. Sueiras, D. Tichit, B. Coq, *Appl. Catal. B* 32 (2001) 167.
- [20] P.G. Simmonds, S. O'Doherty, G. Nickless, G.A. Sturrock, R. Swaby, P. Knight, J. Ricketts, G. Woffendin, R. Smith, *Anal. Chem.* 67 (1995) 717.
- [21] A. Venugopal, K.S. Rama Rao, P.S. Sai Prasad, P. Kanta Rao, *J. Chem. Soc., Chem. Commun.* (1995) 2377.
- [22] E. Kemnitz, A. Hess, G. Rother, S. Troyanov, *J. Catal.* 159 (1996) 332.
- [23] S. Kato, K. Josek, E. Taglauer, *Vacuum* 42 (1991) 253.
- [24] M. Boudart, H.S. Hwang, *J. Catal.* 13 (1975) 44.
- [25] S.T. Srinivas, P. Kanta Rao, *J. Catal.* 148 (1994) 470.
- [26] J.S. Noh, J.A. Schwarz, *Carbon* 28 (1970) 133.
- [27] A.S. Arico, V. Antonucci, L. Pino, P.L. Antonucci, N. Girdano, *Carbon* 28 (1990) 599.
- [28] N. Krishnan Kutty, M.A. Vannice, *J. Catal.* 155 (1995) 312.
- [29] N. Krishnan Kutty, M.A. Vannice, *Appl. Catal. A* 173 (1998) 137.
- [30] S. Deshmukh, J.L. d'Itri, *Catal. Today* 40 (1998) 377.
- [31] G. Fagherazzi, A. Beneditti, S. Polizzi, A. Di Mario, F. Pinna, M. Signoretto, N. Pernicone, *Catal. Lett.* 32 (1995) 293.
- [32] P. Claus, H. Berndt, C. Mohr, J. Radmik, E.-J. Shin, M.A. Keane, *J. Catal.* 192 (2000) 88.
- [33] A. D'Ercole, E. Giamello, C. Pisani, L. Ojamae, *J. Phys. Chem. B* 103 (1999) 3872.
- [34] Y.Z. Chen, C.M. Hwang, C.W. Liaw, *Appl. Catal. A* 169 (1998) 207.
- [35] T. Itoh, M. Kuramoto, M. Yoshida, T. Tokuda, *J. Phys. Chem.* 87 (1983) 4411.